INTERNATIONAL JOURNAL FOR NUMERICAL AND ANALYTICAL METHODS IN GEOMECHANICS, VOL. 21, 153–174 (1997)

BEYOND FAILURE IN GRANULAR MATERIALS

WEI WU[1,*] AND ANDRZEJ NIEMUNIS[2]

[1] *Lahmeyer International Ltd., 60528 Frankfurt a.M., Germany*
[2] *Geotechnical Department, Technical University of Gdańsk, Gdańsk, Poland*

SUMMARY

Recent investigations on the hypoplastic constitutive model for granular materials show that the failure surface can be surpassed by some stress paths. This is contradictory to the conventional definition of failure surface in plasticity, according to which the stress is allowed to move on the failure surface but never across it. In the present paper, the interrelations among the different constitutive models are discussed with special reference to failure and stability. For the hypoplastic constitutive equation, the accessible stress states and the stable stress states are found to be enclosed by a bound surface and a stability surface in the stress space, respectively. Theoretical findings about the bound surface and the stability surface are verified qualitatively by presenting results of triaxial tests on dry sand. © 1997 by John Wiley & Sons, Ltd.

Int. j. numer. anal. methods geomech., vol. 21, 153–174 (1997)
(No. of Figures: 13 No. of Tables: 0 No. of Refs: 41)

Key words: constitutive model; hypoplasticity; failure; stability; granular material

INTRODUCTION

Traditionally, prediction of the behaviour of granular materials has been performed almost exclusively within the framework of plasticity theory. While this approach has achieved certain success, some fundamental issues still remain moot, particularly in view of its application to granular materials, e.g. decomposition of deformation into elastic and plastic parts, transition between elastic and plastic deformation and the use of switch functions to differentiate between loading and unloading. There have been a number of attempts to remedy one or two of the aforementioned aspects by modifying the plastic models. A careful inspection of the relevant literature shows, however, that these shortcomings can be hardly circumvented within the plasticity theory without sacrificing simplicity of the models.

Recently, use of the hypoplastic constitutive model to predict the behaviour of granular materials has been considered in several articles.[1–11] Based on non-linear tensorial functions, the hypoplastic model differs substantially from the plastic models in that the key concepts in plasticity, such as yield surface, flow rule and decomposition of deformation into elastic and plastic parts, are not used in developing the constitutive model. Despite its simplicity the hypoplastic model has been shown to be capable of capturing some salient features of granular materials, such as non-linear and irreversible deformation, dilatancy and coupling between deviatoric and volumetric components of stress and strain. While simulation of various laboratory tests has been accentuated in our past publications, some problems of general interests, e.g.

* Correspondence to: W. Wu, Lahmeyer International Ltd., 60528 Frankfurt a.M., Germany

CCC 0363–9061/97/030153–22$17.50

Received 12 October 1995
Revised 6 June 1995

failure, accessible stress states and stability failed to receive deserved attention. The study of these problems is of interest on two accounts. First, the results may bring out some properties common to plastic and hypoplastic approaches. This will help to foster useful cross-linkages among the theories. Second, the analysis may provide a well founded basis for the finite element implementation of the model.[1,2]

Central to the hypoplastic formulation is incremental non-linearity, which entails a non-linear dependence between stress rate and strain rate. It turns out that the incremental non-linearity has far-reaching consequences for failure and stability. Both the results gained and the methods applied in the present investigation are virtually different from their counterparts in plasticity theory. While our leit-motiv is the study of failure and stability in the hypoplastic model, the theoretical analysis is supplemented by laboratory tests to provide qualitative verifications.

Our presentation opens with a résumé of the hypoplastic constitutive model in Section 2 followed by a classification of constitutive models in Section 3, where the existence of a potential function serves as a touchstone for the classification. The significance of this classification will become apparent in the discussion about failure and invertibility in Section 4. The finding that the failure surface can be surpassed for specific stress paths gives rise to the investigation on accessible stress states and their bound in Section 5. Section 5 is accomplished with the experimental verification of the fact that the failure surface can be surpassed. The final section is devoted to the investigation of stability with respect to the second-order work density.

2. OUTLINE OF HYPOPLASTIC CONSTITUTIVE MODEL

We are concerned here with the following hypoplastic constitutive model proposed by Wu and Kolymbas:[2]

$$\mathring{\mathbf{T}} = \mathsf{L}(\mathbf{T}) : \mathbf{D} + \mathbf{N}(\mathbf{T}) \| \mathbf{D} \| \tag{1}$$

where $\mathbf{T}$ stands for the Cauchy stress, $\mathring{\mathbf{T}}$ the Jaumann stress rate and $\mathbf{D}$ the stretching. The definition of $\mathring{\mathbf{T}}$ and $\mathbf{D}$ can be readily found in textbooks of continuum mechanics, e.g. Reference 13. $\mathsf{L}(\mathbf{T}) : \mathbf{D}$ and $\mathbf{N}(\mathbf{T})$ in (1) are isotropic tensor-valued functions. L is a fourth-order tensor and the colon : denotes an inner product between two tensors, $\| \cdot \|$ stands for a norm and is defined by $\| \mathbf{D} \| = \sqrt{(\mathbf{D} : \mathbf{D})}$. The following notation will be used throughout the paper: bold lowercase and uppercase letters are used to denote vectors and tensors.

Granted that the behaviour to be described is rate independent, constitutive equation (1) is necessarily positively homogeneous of the first degree in $\mathbf{D}$. To show the difference between hypoplasticity and plasticity in more detail, constitutive equation (1) can be recast in a more convenient form by virtue of Euler's theorem for homogeneous functions

$$\mathring{\mathbf{T}} = (\mathsf{L} + \mathbf{N} \otimes \vec{\mathbf{D}}) : \mathbf{D} \tag{2}$$

where $\vec{\mathbf{D}} = \mathbf{D} / \| \mathbf{D} \|$ stands for the direction of stretching, and the symbol $\otimes$ denotes an outer product between two tensors.

Constitutive equation (1) can be regarded *pro forma* as the sum of a linear part and a non-linear part. The two terms in the brackets in (2) represent the tangential stiffness tensor. It is apparent from (2) that the tangential stiffness tensor depends not only on stress but also on the direction of stretching. As compared with plasticity theory, hypoplastic constitutive models are incrementally non-linear. Note that the distinction between loading and unloading is not of importance for the hypoplastic constitutive equation, since the non-linear part is always present irrespective of the

direction of strain rate. As a matter of fact, the determination of the yield surface for granular materials is usually rather subjective, since the stress–strain curves generally do not show clear yielding points as many metallic materials. As will be shown, the incremental non-linearity as given by (1) has significant consequence for the study on failure and stability.

Though the analyses to be presented are not restricted to a specific version of the hypoplastic constitutive model, we will take the following constitutive equation as a heuristic example:[5]

$$\mathring{\mathbf{T}} = C_1(\mathrm{tr}\,\mathbf{T})\mathbf{D} + C_2\frac{(\mathbf{T}:\mathbf{D})\mathbf{T}}{\mathrm{tr}\,\mathbf{T}} + \left(C_3\frac{\mathbf{T}^2}{\mathrm{tr}\,\mathbf{T}} + C_4\frac{\mathbf{T}_\mathrm{d}^2}{\mathrm{tr}\,\mathbf{T}}\right)\|\mathbf{D}\| \tag{3}$$

where C_i $(i = 1, \ldots, 4)$ are dimensionless material parameters. The trace of a tensor is denoted as tr. The deviatoric stress tensor in (3) is defined by $\mathbf{T}_\mathrm{d} = \mathbf{T} - 1/3(\mathrm{tr}\,\mathbf{T})\mathbf{1}$ with $\mathbf{1}$ being the unit tensor. The following constants are found for dense Karlsruhe medium sand with an initial void ratio of about 0·5:[7] $C_1 = -106{\cdot}5$, $C_2 = -801{\cdot}5$, $C_3 = -797{\cdot}1$, $C_4 = 1077{\cdot}7$.

Hypoplastic constitutive equation (3) has been employed successfully to describe various aspects of the behaviour of granular materials. In particular, remarkable progress was achieved recently by Wu,[5] Wu and Bauer[6] and Wu *et al.*[10] by integrating the critical state into hypoplastic constitutive equation (3). The augmented constitutive model covers a broad range of stress level and the whole density spectrum from the loosest to the densest packing and accounts for both initial deformation and fully developed flow. For the sake of simplicity, the analyses are to be performed for constitutive equation (3) without the critical state. Nevertheless, the method developed here can be applied with equal force to the hypoplastic model endowed with the critical state.

3. CLASSIFICATION OF CONSTITUTIVE MODELS

In order to show the position of hypoplasticity in the midst of constitutive models, the following classification and terminology are proposed along the line of work by Hill.[4] Consider a material element under uniform stress and subjected to a closed strain circuit. We proceed to classify the constitutive models according to the recovery of stress at the end of strain circuit and whether the constitutive equation admits a potential.

1. *Hyperelasticity*: A constitutive model is said to be hyperelastic if the stress is recovered on all strain circuits. The stress rate and strain rate are related through an elastic potential. Owing to the existence of the elastic potential there exists a unique relation between stress and strain. The behaviour described by a hyperelastic constitutive equation is path independent. Note that the stress–strain relation need not be linear.
2. *Hypoelasticity*: The stress rate and strain rate in a hypoelastic constitutive equation, as introduced by Truesdell,[15] are related through a tensorial function

$$\mathring{\mathbf{T}} = \mathsf{L}(\mathbf{T}):\mathbf{D} \tag{4}$$

which need not be derivable from a potential. The behaviour described by a hypoelastic constitutive equation is in general path dependent. The stress is recoverable only on special strain circuits, e.g. with zero enclosed area. This can easily be seen from the fact that $\mathring{\mathbf{T}}$ and $-\mathring{\mathbf{T}}$ are obtained by setting $\mathbf{D}$ and $-\mathbf{D}$ into (4). Hypoelastic constitutive equations are incrementally linear in the sense that the tangential stiffness tensor depends only on stress. Applications of hypoelastic constitutive models to granular materials has been shown among others by Stutz,[16] Romano[17] and Davis and Mullenger.[18]

3. *Hyperplasticity*: By hyperplasticity we mean constitutive models rested upon plasticity theory admitting plastic potentials. Usually, two or more equations, representing different branches of the stress–strain behaviour for loading and unloading, are employed in hyperplastic models. As a consequence, switch functions are needed to distinguish between the different branches. The stress at the end of the strain circuit is recovered for the one branch and is not recovered for the other. Hyperplastic constitutive equations are sometimes called bilinear or multi-linear models in the sense that the relation between the stress rate and strain rate is linear within distinct sectors in the stress or strain space.
4. *Hypoplasticity*: No plastic potential is used in the hypoplastic model and the relation between stress rate and strain rate is incrementally non-linear in the sense that no matter how small the strain rate may be the behaviour is always path dependent.

4. FAILURE SURFACE AND INVERTIBILITY CONDITION

The subject of concern is the so-called homogeneous failure, i.e. failure under uniform stress and homogeneous strain, predicted by the constitutive model. The so-called localized failure in form of shear band is not within the scope of the investigation here and has been treated elsewhere.[4]

A material element is said to be at failure if further straining results in no variation in stress. The above statement can be put in a stringent way as follows:

A material element under stress $\mathbf{T}$ is at failure if there exists $\mathbf{D} \neq \mathbf{0}$ such that

$$\mathring{\mathbf{T}} = \mathbf{0} \tag{5}$$

The stretching $\mathbf{D}$ satisfying (5) characterizes the flow rule. Failure is described by the pair $(\mathbf{T}, \mathbf{D})$. On the failure surface there exists at least one $\mathbf{D}$ such that the stress rate vanishes. Before proceeding further it is useful to introduce the so-called stiffness locus[19] or response envelope.[20] Owing to the complexity of the most constitutive equations, the property of a constitute equation can hardly be detected thoroughly in an analytical way. In general, comparison between predictions and laboratory tests provides only limited information along restricted stress paths. As such, numerical methods are often resorted to bring out the important features of the constitutive models. The stiffness locus has been proved to be an efficient instrument to study the behaviour of the constitutive equations.

The stiffness locus at a given stress state $\mathbf{T}_0$, called *initial stress*, is the surface spanned by all stress rates $\mathring{\mathbf{T}}$ which result from the corresponding probes of the stretching $\mathbf{D}$ with the same magnitude $\|\mathbf{D}\|$. The stiffness loci can be presented either in the space of stress rate or in the stress space by adding the stress increment to the initial stress $\mathbf{T} = \mathbf{T}_0 + \dot{\mathbf{T}}\,\Delta t$. To visualize the results, let us consider a triaxial stress state with $T_2 = T_3$. In this case, the stiffness loci can be represented on the planes T_1–T_2 and D_1–D_2 with the indices 1, 2 and 3 for the principal stresses, see Figure 1.

The following properties of the stiffness locus are useful in the discussion about failure. For details the reader is referred to Wu and Kolymbas.[2]

(a) The distance from a point on the stiffness locus to the point of the initial stress characterizes the tangential stiffness for a given direction of stretching (directional stiffness). It is therefore clear that the stiffness locus passes through the initial stress at failure since the tangential stiffness at failure must vanish for at least one direction of stretching.
(b) The stiffness locus of the hyper- and hypoelastic constitutive equations is an ellipse with the initial stress in its centre. That the initial stress must be in the centre of the stiffness loci can easily be shown by the fact that the responses of a hyper- or hypoelastic constitutive

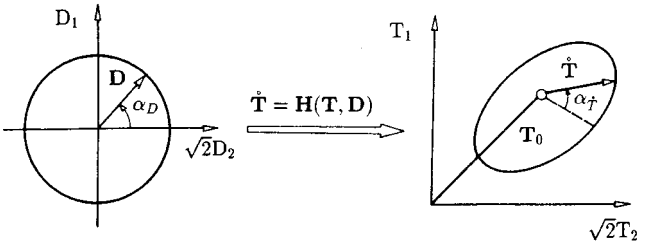

Figure 1. Principal sketch of stiffness locus on the T_1–T_2 plane

equation for two stretchings of the same length (norm) and in opposite directions, $\mathbf{D}$ and $-\mathbf{D}$, are also of the same length (norm) and in opposite directions, $\mathring{\mathbf{T}}$ and $-\mathring{\mathbf{T}}$. This is only possible if the initial stress lies in the centre of the stiffness locus. The complete proof can be found in the work by Wu and Kolymbas.[2]

(c) The stiffness locus of hypoplastic constitutive equation (1) is an ellipse whose position is shifted with reference to the initial stress. This property of the stiffness locus pertinent to hypoplasticity can readily be seen by the fact that constitutive equation (1) is composed of a linear and a non-linear part and the non-linear part depends on stretching only through its norm $\|\mathbf{D}\|$. Since $\|\mathbf{D}\|$ remains constant for a stiffness locus, the response of the non-linear part is independent of the direction of stretching and results in a translation of the elliptical stiffness locus.

In passing, the stiffness loci need not be convex since such a restriction follows neither from the requirement of uniqueness nor from the consideration of any work inequality. The only requirement on the shape of the stiffness loci is that the region enclosed by the stiffness locus should be simply connected.[21,2]

It remains to point out that the above properties of the stiffness loci on the plane T_1–T_2 can easily be generalized to multidimension. In this case the stiffness loci of the hyper- and hypoelastic constitutive equations are ellipsoids in lieu of ellipses.

4.1. Hypoelasticity

The so-called hypoelastic yielding, which is in our context failure, was first investigated by Truesdell.[15] However, it was not until Tokuoka[22] that the general failure criterion for the hypoelastic constitutive equations was laid down. Consider hypoelastic constitutive equation (4). For vanishing stress rate we have

$$\mathring{\mathbf{T}} = \mathsf{L} : \mathbf{D} = \mathbf{0} \tag{6}$$

From the condition $\mathbf{D} \neq 0$ in the above equation it follows that the determinant of L must vanish:

$$\det \mathsf{L} = 0 \tag{7}$$

Note that the hypoelastic constitutive equation is not invertible under condition (7) and the failure condition is equivalent to the loss of invertibility. The flow rule resulting from (6) is determined by the eigenvector.

We turn to investigate failure of hypoelastic constitutive equations with the help of the stiffness locus. For triaxial stress states, the stiffness locus of a hypoelastic constitutive equation is an

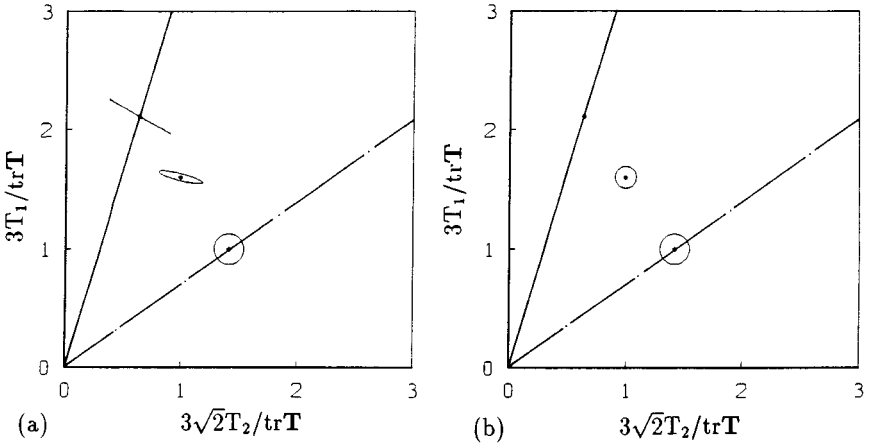

Figure 2. Typical stiffness loci of hypoelastic constitutive equations: (a) the stiffness locus degenerates to a line segment at failure and (b) the stiffness locus degenerates to a point at failure

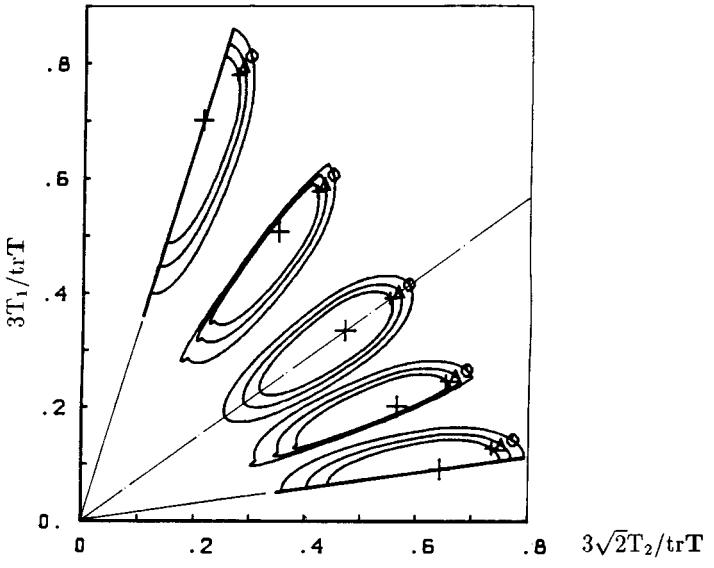

Figure 3. Stiffness loci of the hyperplastic constitutive model proposed by Vermeer[38]

ellipse with the initial stress in the centre. Furthermore, the stiffness locus at failure must go through the initial stress. It follows that this is only possible if the elliptical stiffness locus degenerates to a line segment or a point. In the former case the stress rate vanishes only for two specific directions of stretching, while for the latter case the stress rate vanishes identically for all directions of stretching. This is demonstrated with two specific hypoelastic constitutive equations in Figure 2. In passing, if the stress rate vanishes for all **D**, as shown in Figure 2(b), the stress is locked, i.e. the stress state at failure cannot be left after it is reached. This property of the hypoelastic model must be regarded as pathological.

4.2. *Hyperplasticity*

In hyperplasticity (plasticity), failure is specified *a priori* by a failure surface. Since more than one stress–strain relation is involved, one for loading and one for unloading, the stiffness locus is composed of several segments. This can clearly be observed from Figure 3. If the consistency condition is fulfilled the stiffness loci will be continuous but generally not smooth. However, the stiffness loci can be made smooth by choosing a specific flow rule.[23] When the stress is approaching the failure surface, one segment of the stiffness locus corresponding to loading becomes flatter and coincides eventually with the failure surface. The stress–strain relations, though different for loading and unloading, are incrementally linear as long as loading or unloading is known. At failure the matrix of tangential stiffness corresponding to loading becomes singular, which corresponds to the loss of invertibility of the hyperplastic equation.

The stiffness loci are composed of segments of two or more ellipses. The compatibility condition guarantees the continuous transition from loading to unloading through the so-called neutral loading. The initial stress lies again in the centre of the ellipses. At failure the segment for loading degenerates to a line segment with the initial stress in the middle. Apparently, for the so-called loading to the side the prediction by the hyperplastic constitutive equations will give a too stiff response. There have been some modifications reported in the literature to make the response for the loading to the side 'softer', e.g. the stress vertex theory by Batdorf and Budiansky.[24]

After failure surface is reached, the stress is allowed to move on the failure surface upon further loading but not across it as a consequence of the consistency condition. In other words, the failure surface bounds all accessible stress states.

4.3. *Hypoplasticity*

Referring to constitutive equation (1), we proceed to derive explicit expressions of the failure surface and the flow rule. For vanishing stress rate we have

$$\mathring{\mathbf{T}} = \mathsf{L} : \mathbf{D} + \mathbf{N} \| \mathbf{D} \| = \mathbf{0} \tag{8}$$

The above equation is an isotropic tensorial relation between the dynamical and kinematical quantities, $\mathbf{T}$ and $\mathbf{D}$. Due to rate independence, equation (8) is necessarily homogeneous of zero degree in $\mathbf{D}$. Previous investigations by Sawczuk and Stutz[25] indicate that the requirement of the rate independence imposes a scalar function on stress. This function characterizes the failure surface.

Let us first consider the flow rule at failure, namely the direction of stretching corresponding to the vanishing stress rate. Since the stretching in concern is other than zero, equation (8) can be divided by the norm of stretching to give

$$\frac{\mathbf{D}}{\| \mathbf{D} \|} = - \mathsf{L}^{-1} : \mathbf{N} \tag{9}$$

Note that only the direction of stretching at failure is specified by equation (8) and there is no one-to-one correspondence between $\mathring{\mathbf{T}}$ and $\mathbf{D}$ at failure.

By making use of the definition of the norm $\| \mathbf{D} \|$ we obtain

$$\frac{\mathbf{D} : \mathbf{D}}{\| \mathbf{D} \|^2} = 1 \tag{10}$$

Substitution of (9) into (10) leads to the expression for the failure surface:

$$f(\mathbf{T}) = \mathbf{N}^{\mathrm{T}} : (\mathsf{L}^{-1})^{\mathrm{T}} : \mathsf{L}^{-1} : \mathbf{N} - 1 = 0 \tag{11}$$

where the superscript T denotes the transposition of a tensor.

From the above derivations it may be seen that failure concerns two aspects, namely kinematical and dynamical. Consequently, there are two equations which follow from the definition of failure. The first one specifies the direction of stretching at failure and is called the flow rule while the second one concerns the stress at failure and is termed the failure surface. It is worth noting that the failure surface and the flow rule in hypoplasticity emerge as *by-products* of the constitutive equation, whereas in hyperplasticity they are generally to be prescribed *a priori*, e.g. the Mohr–Coulomb failure surface with the associated or non-associated flow rule.

A further remark is relevant to whether the flow rule (9), with reference to the failure surface (11), is associated. A perusal of (9) and (11) suggests that the flow rule is non-associated, since in general $\partial f(\mathbf{T})/\partial \mathbf{T} \neq -\mathsf{L}^{-1} : \mathbf{N}$. A noteworthy case is when the non-linear term $\mathbf{N}(\mathbf{T})$ in constitutive equation (1) is dropped. In this case the hypoelastic constitutive equation (4) is recovered. It can be seen that the failure condition in hypoelasticity can be regarded as a special case in hypoplasticity.

Consider now the invertibility of hypoplastic constitutive equation (1). It is assumed that L in (1) is always positively definite. Taking stretching $\mathbf{D}$ as the unknown, we try to solve constitutive equation (1) for $\mathbf{D}$. Denoting $\mathbf{A} = \mathsf{L}^{-1} : \mathring{\mathbf{T}}$ and $\mathbf{B} = \mathsf{L}^{-1} : \mathbf{N}$, $x = \|\mathbf{D}\|$, we find from constitutive equation (1) that

$$\mathbf{D} = \mathbf{A} - x\mathbf{B} \tag{12}$$

The scalar x in the above equation can be found from the following quadratic equation:

$$\mathbf{D} : \mathbf{D} = x^2 = (\mathbf{A} - x\mathbf{B}) : (\mathbf{A} - x\mathbf{B}) \tag{13}$$

The solutions of the above equation can be written out explicitly:

$$x_{1,2} = \frac{\mathbf{A} : \mathbf{B}}{\mathbf{B} : \mathbf{B} - 1} \pm \sqrt{\left(\frac{\mathbf{A} : \mathbf{B}}{\mathbf{B} : \mathbf{B} - 1}\right)^2 - \frac{\mathbf{A} : \mathbf{A}}{\mathbf{B} : \mathbf{B} - 1}} \tag{14}$$

The inversion of (1) is completed by substituting (14) into (12). Obviously, only positive root $x = \|\mathbf{D}\|$ is admitted. Therefore, if $x_1 \cdot x_2 > 0$ the inverse solution does not exist or is not unique. This statement is the criterion of invertibility of constitutive equation (1). Making use of (14) we may write this criterion in a simpler form

$$\mathbf{B} : \mathbf{B} < 1. \tag{15}$$

The above expression is equivalent to the failure condition as given in (11).

The failure surface calculated from constitutive equation (3) is shown on a deviatoric plane in Figure 4(a) together with the experimental data on Karlsruhe medium sand obtained with a true triaxial apparatus.[26] Owing to the fact that constitutive equation (3) is homogeneous of the first degree in $\mathbf{T}$, the tangential stiffness is proportional to tr $\mathbf{T}$ and the friction angle is independent of tr $\mathbf{T}$. In the principal stress space, the failure surface is a cone with the apex at the origin of the co-ordinate system (T_1, T_2, T_3). The calculated flow rule is shown on a deviatoric plane in Figure 4(b) together with the failure surface. A visual inspection of Figure 4(b) indicates that the derived flow rule is non-associated.

Since the non-linear term in constitutive equation (1) depends only on the norm of stretching and not on its direction, the stiffness locus is translated with the reference to the initial stress. The

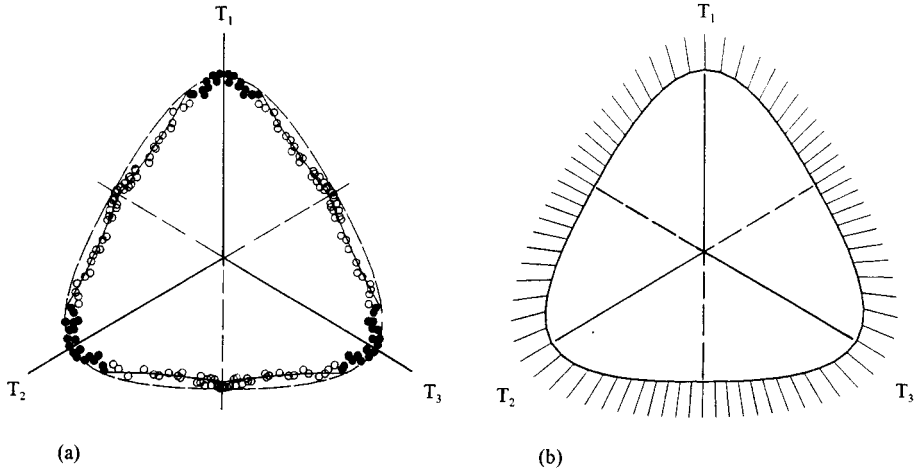

Figure 4. Failure surface and flow rule obtained with constitutive equation (3): (a) failure surface on a deviatoric plane; (b) flow rule on a deviatoric plane

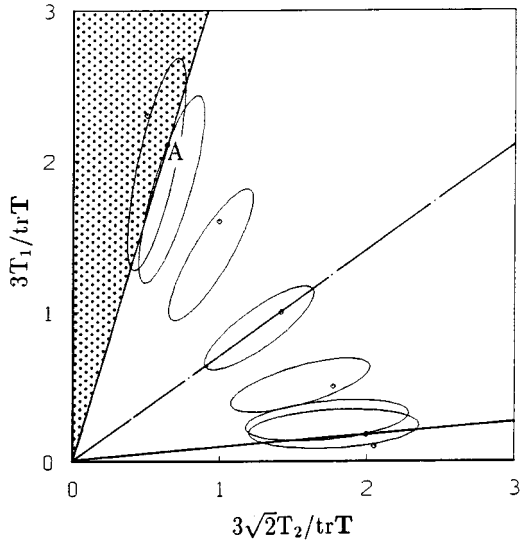

Figure 5. Stiffness loci of hypoplastic constitutive equation (3)

shape and orientation of the stiffness locus are fully determined by the linear term. At failure, the translation due to the non-linear term is so large that the stiffness locus passes through the initial stress. It can be anticipated that the behaviour for loading to the side predicted by a hypoplastic model will be softer than that of a hyperplastic model.

The stiffness loci obtained with constitutive equation (3) are depicted in Figure 5 together with the failure surface. We observe from Figure 5 that the failure surface intersects the stiffness locus at failure. A small portion of the stiffness locus lies outside the failure surface. This means that by choosing specific stress paths the failure surface can be surpassed. In other words, the failure

surface does not coincide with the bound of the accessbile stress states. This finding is quite surprising since it contradicts the classical concept of failure. In the next section, we will investigate whether there exists a bound surface enclosing all accessible stress states for constitutive equation (3).

5. ACCESSIBLE STRESS STATES AND BOUND SURFACE

As shown in Section 4, some stress paths may lead to stress states beyond the failure surface. We proceed to investigate whether the accessible stress states are bounded by a bound surface, which separates the accessible stress states from the inaccessible. For constitutive equation (3) we will show that such a bound surface exists. In Figure 6 the bound surface obtained with constitutive equation (3) is shown on a deviatoric plane. The bound surface possesses similar geometry to the failure surface and lies slightly outside the failure surface.

The bound surface is an intrinsic property of hypoplastic constitutive equation (3), which means that we do not need any return algorithms as is the case in most hyperplastic models to correct the drift of stress during the numerical integration.[27] The stress states lying outside the bound surface, e.g. as a result of too large time increment, will be automatically corrected in the next time step. In what follows, a numerical scheme is described to find the bound surface. Moreover, some experiments supporting the theoretical finding are presented.

5.1. *Theoretical analysis*

We set off with the assumption that there exists a bound surface $b(\mathbf{T}) = 0$ with $b(\mathbf{T})$ being an isotropic function of stress. Consider the stress $\mathbf{T}^*$ which happens to be on the bound surface so that $b(\mathbf{T}^*) = 0$. The outward normal to the bound surface at $\mathbf{T}^*$ is per definition

$$\mathbf{Z} = \left.\frac{\partial b(\mathbf{T})}{\partial \mathbf{T}}\right|_{\mathbf{T}=\mathbf{T}^*} \tag{16}$$

It is convenient to represent the stress $\mathbf{T}^*$ by its three principal components, i.e. in its diagonal form. The outward normal $\mathbf{Z}$ can be shown to be diagonal as well.

According to the definition of the bound surface all stress rates $\mathring{\mathbf{T}}$ calculated at $\mathbf{T}^*$ must be directed to the interior of the bound surface so that for any strain rate $\mathbf{D}$ the corresponding stress rate $\mathring{\mathbf{T}}$ must satisfy the inequality

$$\mathbf{Z} : \mathring{\mathbf{T}} \leqslant 0 \tag{17}$$

Since $\mathbf{Z}$ is diagonal, we need only consider the diagonal components of $\mathring{\mathbf{T}}$ and $\mathbf{Z}$ when evaluating their product in the above inequality. Thus, without loss of generality, we may consider only the stress rates coaxial with the stress $\mathbf{T}^*$. From inequality (17) it follows that if the stress state lies on the bound surface then the maximum of the scalar product must vanish, i.e.

$$\max(\mathbf{Z} : \mathring{\mathbf{T}})_{\mathbf{T}=\mathbf{T}^*} = 0 \tag{18}$$

Substituting constitutive equation (1) into (18) and differentiating the resulting equation after $\mathbf{D}$ leads to the following condition for maximizing $\mathbf{Z} : \mathring{\mathbf{T}}$:

$$\frac{\partial [\mathbf{Z} : \mathsf{L} : \mathbf{D} + \mathbf{Z} : \mathbf{N} \| \mathbf{D} \|]}{\partial \mathbf{D}} = \mathbf{Z} : \mathsf{L} + \mathbf{Z} : \mathbf{N} \frac{\mathbf{D}}{\| \mathbf{D} \|} = \mathbf{0} \tag{19}$$

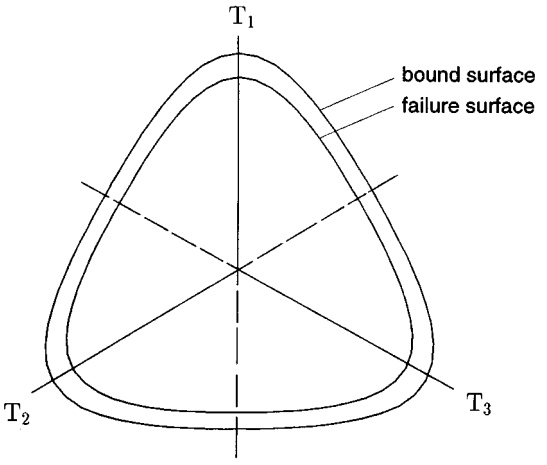

Figure 6. Cross-section of the failure surface and the bound surface on a devoatoric plane obtained with hypoplastic constitutive equation (3)

Since the constitutive equation in concern is rate independent we may set $\|\mathbf{D}\| = 1$. The stretching maximizing the product $\mathbf{Z}:\mathring{\mathbf{T}}$ can be found from the above equation:

$$\mathbf{D}_{\max} = -\frac{\mathbf{Z}:\mathsf{L}}{\mathbf{Z}:\mathbf{N}} \tag{20}$$

Substituting (20) into (18) we arrive at the following criterion for the stress lying on the bound surface $b(\mathbf{T}) = 0$:

$$(\mathbf{Z}:\mathsf{L}):(\mathbf{Z}:\mathsf{L}) = (\mathbf{Z}:\mathbf{N})^2 \tag{21}$$

It should be noted that this criterion alone, contrary to the failure condition, is not sufficient to determine the bound surface since the outward normal $\mathbf{Z}$ still remains unknown.

The problem of determining the outward normal $\mathbf{Z}$ can be resolved by taking into account that the constitutive relation (1) is positively homogeneous of the first degree in stress and that the bound surface is an isotropic function of stress. By way of the definition of positive homogeneity we have for any scalar $\alpha > 0$

$$\mathring{\mathbf{T}}(\alpha\mathbf{T}, \mathbf{D}) = \alpha\mathring{\mathbf{T}}(\mathbf{T}, \mathbf{D}) \tag{22}$$

As a consequence, if all stress rates $\mathring{\mathbf{T}}(\mathbf{T}^*, \mathbf{D})$ computed at $\mathbf{T}^*$ satisfy inequality (17) so do all $\mathring{\mathbf{T}}(\alpha\mathbf{T}^*, \mathbf{D})$. Hence, if the stress $\mathbf{T}^*$ lies on the bound surface then also $\alpha\mathbf{T}^*$ does. It follows from the homogeneity of the constitutive equation in stress that the bound surface $b(\mathbf{T}) = 0$ represents a conical surface with the vertex in the origin of the stress space. The above property implies the following condition of orthogonality between $\mathbf{T}^*$ and $\mathbf{Z}$:

$$\mathbf{T}^*:\mathbf{Z} = 0 \tag{23}$$

The assumption that the bound surface is an isotropic function of stress implies that for triaxial stress states $\mathbf{T}^* = \mathrm{diag}(T_1^*, T_2^*, T_3^*)$ with $T_2^* = T_3^*$ the respective partial derivatives, Z_2 and Z_3, must be equal. Making use of this property under consideration of (23) the stress states on the

bound surface $b(\mathbf{T}) = 0$ can be found by solving the following equation system:

$$\begin{gathered} \mathbf{T}^* - \frac{\mathbf{T}^* : \mathbf{T}^*}{\mathbf{T}^* : \mathbf{1}} \mathbf{1} = \mathbf{Z} \\ (\mathbf{Z} : \mathsf{L}) : (\mathbf{Z} : \mathsf{L}) = (\mathbf{Z} : \mathbf{N})^2 \end{gathered} \tag{24}$$

We denote the triaxial stress state $\mathbf{T}^*$ satisfying the above system of equations as $\mathbf{T}_0^*$, which serves as the start point for the determination of the subsequent points on the bound surface. The next point $\mathbf{T}_1^*$ on the bound surface in the vicinity of the stress $\mathbf{T}_0^*$ may be found numerically. Since only the diagonal components are concerned, we may replace the diagonal tensors $\mathbf{T}$ and $\mathbf{Z}$ with the corresponding vectors $\mathbf{t}$ and $\mathbf{z}$ and write out the following generic scheme:

$$\mathbf{t}^{*(i+1)} = \mathbf{t}^{*(i)} + \theta \, \mathbf{t}^{*(i)} \times \mathbf{z} \tag{25}$$

where i is the number of step and θ the step length. The whole cross-section of the bound surface on a deviatoric plane can be found by performing the calculation in (25) stepwise. The bound surface has been discussed by Wu and Kolymbas[2] and Kolymbas.[3] Their method to determine the bound surface is based on the triaxial stress states and does not provide the genuine bound surface for the general stress states. In what follows, the surface determined by their method is termed the pseudo-bound surface. In order to compare the bound surface in the present paper and the pseudo-bound surface, the main ingredients of their method is briefly outlined.

Let us consider the stiffness locus at a given initial stress and search for the stress rates parallel to the initial stress. It is straightforward to show that such stress rates are given by the following equation:

$$\mathring{\mathbf{T}} = \alpha \mathbf{T} \tag{26}$$

where α is an arbitrary scalar. In general, the above equation possesses two distinct solutions for α. The two solutions correspond to the stress rates for loading and unloading. If the above equation possesses two identical solutions, the initial stress lies on the pseudo-bound surface. The stiffness locus at an initial stress on the pseudo-bound surface is tangential to the straight line connecting the initial stress and the origin of the principal stress space. As will be shown below, for the general stress states the pseudo-bound surface is different from the bound surface.

That the failure surface can be surpassed has also been discussed by Chambon *et al.*[28] within their incrementally non-linear model, which possesses similar formulation to constitutive equation (1). Contrary to our approach to find the bound surface, they attempt to force the stress to fulfil the so-called consistency condition, so that the failure surface cannot be surpassed. Judging from the stiffness loci in their paper, their approach seems to be less successful and leads to the pathological stiffness loci as shown in Figure 2(b).

The relative position of the stiffness loci with reference to the failure surface and the bound surface can be best visualized with the help of of a graphical software. In the three-dimensional space of principal stresses the stiffness loci are ellipsoids. A perspective picture of the failure surface and the bound surface is shown in Figure 7 together with two stiffness loci. The initial stresses of the two stiffness loci are chosen to lie on the bound surface and the pseudo-bound surface, respectively. An enlarged portion of Figure 7 is depicted in Figure 8. The stiffness locus on the right shown in Figure 8 is obtained for an initial stress on the bound surface while the initial stress of the left stiffness locus lies the pseudo-bound surface. Figures 8(b) and 8(c) show that the right stiffness locus is tangential to the bound surface. and the left stiffness locus is tangential to

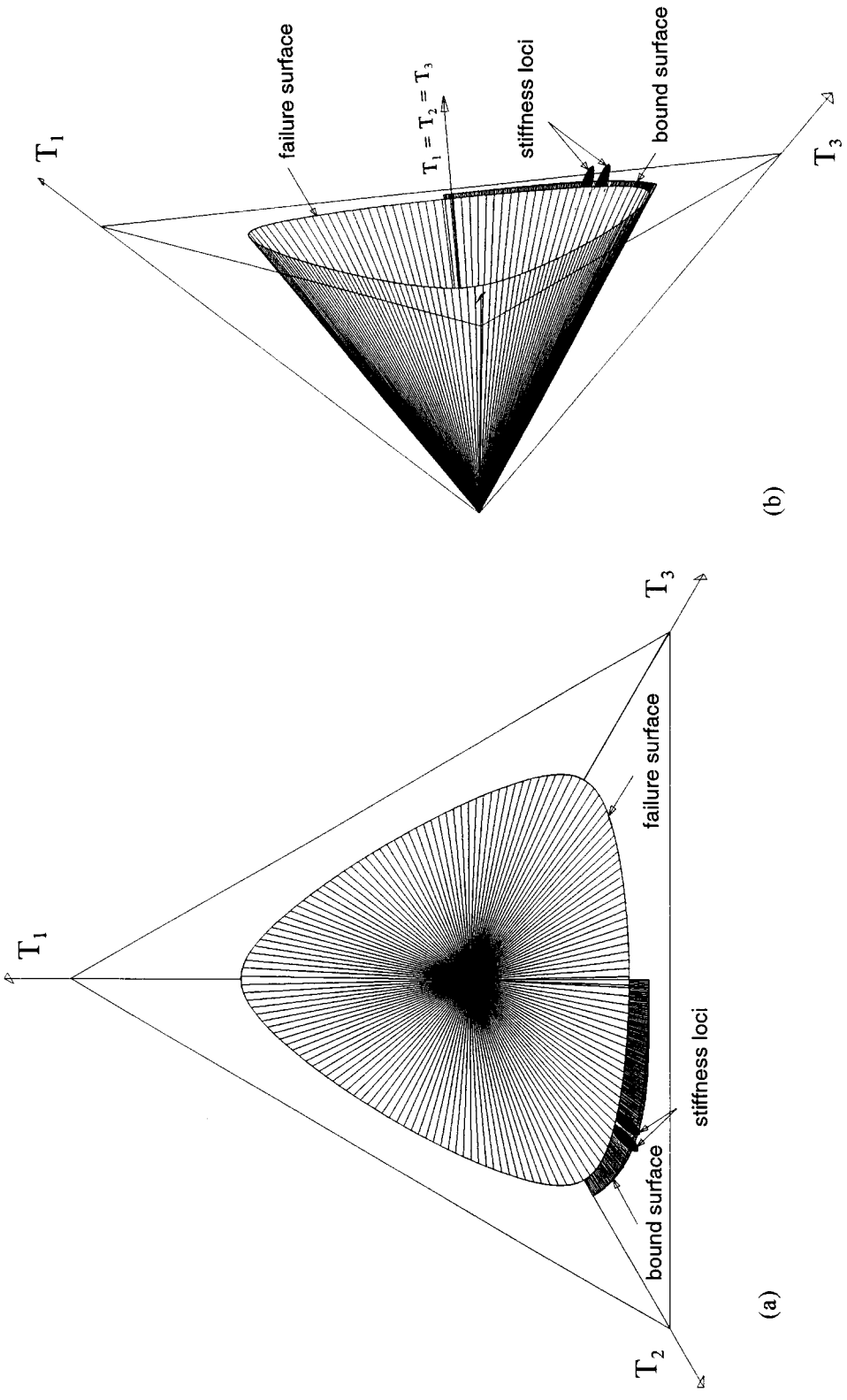

Figure 7. The failure surface, a part of the bound surface and two stiffness loci plotted in principal stress space according to constitutive equation (3)

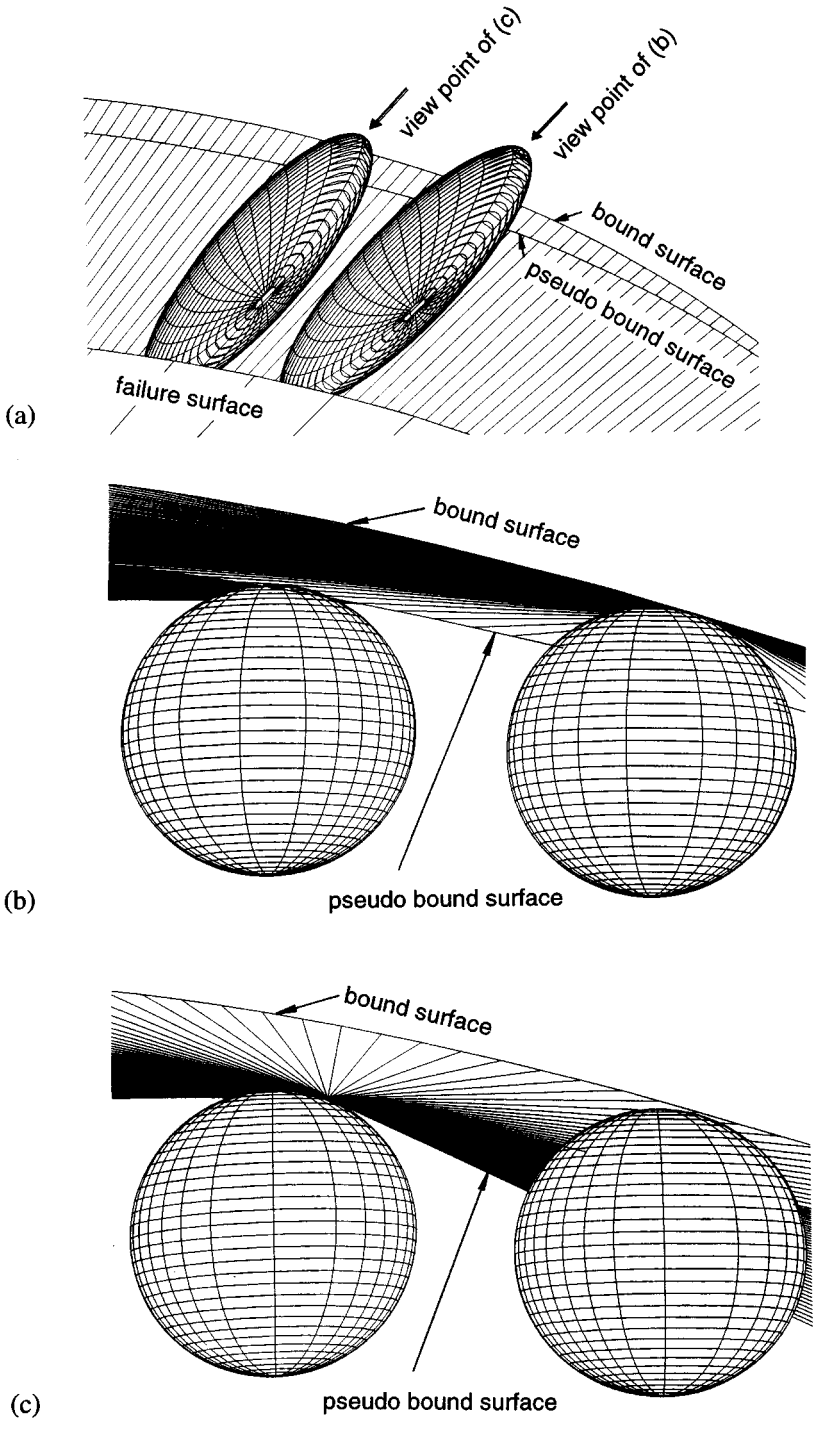

Figure 8. The enlarged portions of Figure 7: (a) the view point is located on the axis with $T_1 = T_2 = T_3$; (b) the view point is located along the direction of the initial stress of the left stiffness locus; (c) the view point is located along the direction of the initial stress of the right stiffness locus

the pseudo-bound surface. It can be seen from Figures 8(b) and 8(c) that the right stiffness locus lies partially outside the pseudo-bound surface. This means that the pseudo-bound surface as determined according to Wu and Kolymbas[2] and Kolymbas[3] can still be surpassed and does not represent the genuine bound surface. This shows also the significance of extending the stiffness loci to the multi-dimensional case.

5.2. *Experimental observation*

So far, the bound surface has been treated theoretically. In order to provide a qualitative verification of the theoretical finding several triaxial tests are carried out. The tests are conducted on dry sand (Karlsruhe medium sand) in the strain-controlled triaxial apparatus described by Wu and Kolymbas.[29] Karlsruhe medium sand is composed mainly of subround quartz grains with $d_{50} = 0{\cdot}3$ mm. The so-called free-ends are used to reduce the influence of end friction. The specimens with an initial void ratio of about 0·5 are prepared by air pluviation of sand through several sieves. In this way, homogeneous specimens of a given density can be reproduced.

Since dry sand is used in tests, the conventional method of radial displacement measurement by inferring radial displacement from the amount of water expelled out of the specimen cannot be applied. The radial displacements are measured directly with three rings of spring-steel placed on the specimen (Figure 9). Four strain gauges are applied on both sides of each ring to form a full

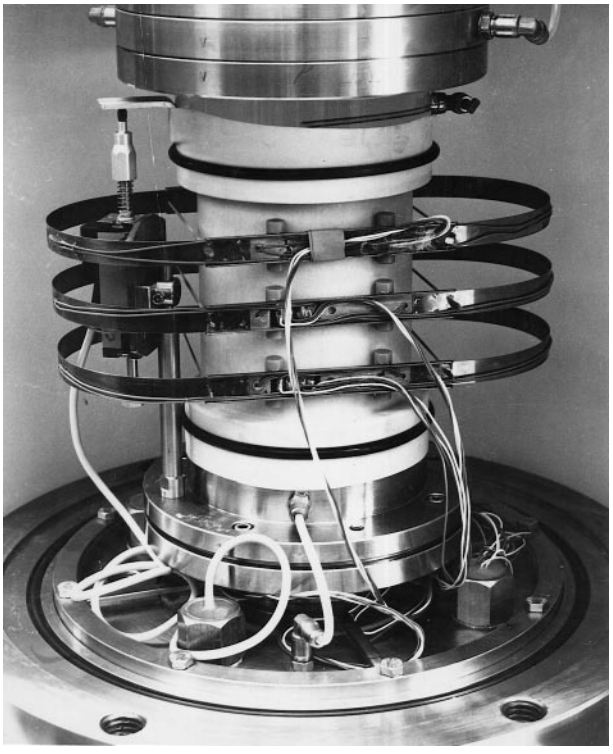

Figure 9. Specimen with rings mounted for the measurement of radial displacement

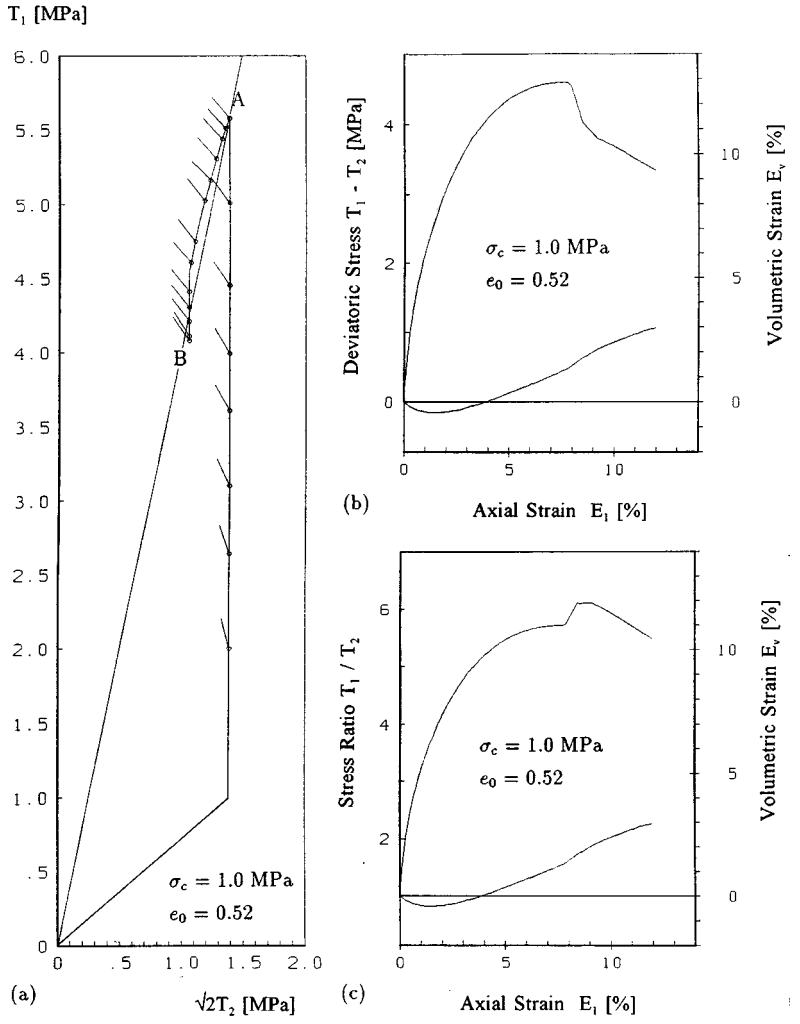

Figure 10. Triaxial compression test on a specimen of dense sand: (a) stress path; (b) stress difference over axial strain; (c) stress ratio over axial strain

bridge. An accuracy of 0.01 mm can be achieved. A distinct advantage of the rings is the possibility to detect inhomogeneous deformation during the test.

The test process is servo-controlled by a computer. For a given stress path a comparison between the actual and the required value is made in a given time interval. If the difference exceeds the tolerance, the confining pressure will be varied by a computer controlled valve. The stress path is approximated by a number of straight segments.

Figure 10 shows a typical triaxial test. The stress path together with the direction of strain increment along the stress path is depicted in Figure 10(a). In Figures 10(b) and 10(c) the stress–strain curves and the volumetric strain curves are given. The specimen is first brought to a hydrostatic stress of $\sigma_c = 1{\cdot}0$ MPa ($T_1 = T_2 = \sigma_c$) and then loaded by increasing the axial

stress while keeping the radial stress constant until failure (point A) is reached, which can be inferred from the plateau of the stress–strain curves in Figures 10(b) and 10(c). If the stress path is kept unchanged, the stress will remain stationary or show moderate strain softening with further straining. For the test in Figure 10, the stress path is changed at point A following $A \Rightarrow B$. Different stress paths are probed until the increase of the stress ratio T_1/T_2 reaches its maximum.

The following observations can be made from Figure 10. Along the stress path $A \Rightarrow B$ the stress difference decreases monotonically whereas the stress ratio increases to its maximum and then decreases (Figures 10(b) and 10(c)). The failure surface in this diagram is depicted as the straight line connecting point A and the origin. Clearly, the stress path $A \Rightarrow B$ lies beyond the failure surface. It should be reminded that we do not intend to make a quantitative comparison between the predicted and the experimental results. Rather, the experiments should be regarded as a qualitative verification of the prediction from hypoplastic constitutive equation (3). Another interesting phenomenon can be seen from Figure 10(a). Though there is a drastic change of the direction of stress increment, there is only minor variation of the direction of the strain increment. An increase of the volumetric strain can also be observed in Figure 10(b).

Figure 11 shows the variation of the second-order work density during the test. The second-order work density is evaluated according to $d^2W = \Delta T_1 \Delta E_1 + 2\Delta T_2 \Delta E_2$ with E_1 and E_2 being the axial and radial strain. As might be expected, the magnitude of d^2W depends on the magnitude of the strain increment. For the results in Figure 11 an axial strain increment of $\Delta E_1 \approx 0{\cdot}001$ is used. The second-order work density is seen to decrease from an initially positive value to zero at failure and becomes even negative along the path $A \Rightarrow B$. An ensuing question will be whether it is possible to have $d^2W < 0$ before failure. This problem will be investigated together with the stability surface in the next section.

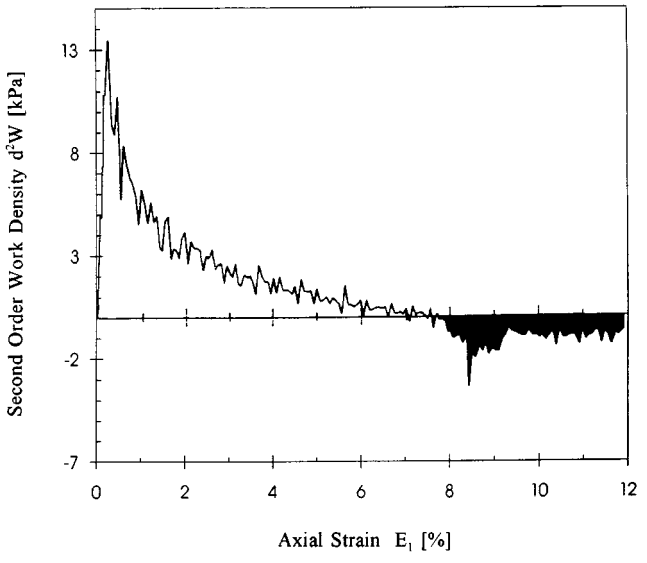

Figure 11. Second-order work density over axial strain obtained from the triaxial compression test in Figure 10

6. STABILITY SURFACE AND STRAIN SOFTENING

In view of the complexity of the non-linear constitutive models, it is desirable to obtain qualitative properties such as existence, stability and uniqueness of the boundary value problems posed with the constitutive models. The qualitative properties can be provided by constitutive inequalities to be fulfilled by the constitutive models. A simple and well-known inequality constrains the stress rate to be directed so that the second-order work density defined by

$$\mathrm{d}^2W = \mathrm{tr}(\mathring{\mathbf{T}}\mathbf{D}) \tag{27}$$

is positive for all directions of stretching.

According to Hill,[14,30,31] the inequality $\mathrm{d}^2W > 0$ is sufficient to guarantee stability. A comprehensive account with illustrative examples on this subject can be found in the recent work by Bazant,[32] who showed that $\mathrm{d}^2W > 0$ is a sufficient condition for stability under dead load. For variable load, however, higher-order terms are to be included in (27). The relevance of $\mathrm{d}^2W > 0$ to uniqueness is less clear. Valanis[33] showed that uniqueness can still be proved even if the above inequality is violated. It should be pointed out that most conclusions arrived at the literature concern the incrementally linear models. Little is known about the validity of such conclusions for incrementally non-linear models.[34] Furthermore, we are concerned here with the so-called material stability or diffuse instability defined by an infinitely small perturbation from an equilibrium state, which is to be differentiated from the loss of stability through localized deformation.[4]

The experiment in the last section shows that the second-order work density can become negative between the failure surface and the bound surface. We proceed to investigate whether d^2W can be negative for constitutive equation (3). To this end, we search for the boundary between positive and negative second-order work density by letting $\mathrm{d}^2W = 0$. If this boundary builds a surface in the stress space, it will be called *stability surface*.

For incrementally linear models, the requirement $\mathrm{d}^2W > 0$ is equivalent to positive definiteness of the tangential stiffness tensor. The proof of positive definiteness can be performed in a straightforward way. The difference between hypoplastic and incrementally linear models can readily be seen by setting constitutive equation (2) into (27) to get the following expression for the stability surface:

$$\mathrm{d}^2W = \mathbf{D} : (\mathsf{L} + \mathbf{N} \otimes \vec{\mathbf{D}}) : \mathbf{D} = 0 \tag{28}$$

Clearly, the above equation is satisfied by the pair $(\mathbf{T}, \mathbf{D})$ at failure. We search for such stress states, for which $\mathring{\mathbf{T}}$ and $\mathbf{D}$ are both non-vanishing and orthogonal. Since the tangential stiffness tensor depends not only on stress but also on the direction of stretching, the problem can only be solved numerically.

The stress state satisfying equation (28) can be found as follows. Starting from a hydrostatic stress state, the second-order work density is calculated for all possible directions of $\mathbf{D}$. It suffices to restrict to the stretching coaxial with the stress. To this end, the stretching $\mathbf{D}$ with $\|\mathbf{D}\| = 1$ can be expressed in a spherical coordinate system as follows:

$$\mathbf{D} = \begin{pmatrix} \cos\zeta \sin\eta & 0 & 0 \\ 0 & \sin\zeta \sin\eta & 0 \\ 0 & 0 & \cos\eta \end{pmatrix}. \tag{29}$$

d^2W is computed by varying ζ in the range $(0^\circ \leqslant \zeta \leqslant 360^\circ)$ and η in the range $(-90^\circ \leqslant \eta \leqslant 90^\circ)$. If d^2W is positive for all directions of $\mathbf{D}$, the deviatoric stress is increased stepwise. The above

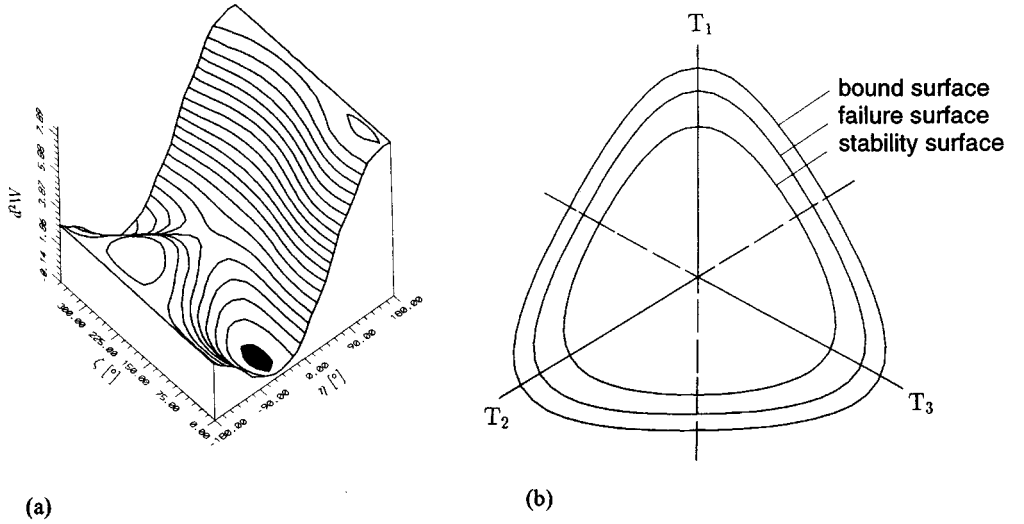

Figure 12. Second-order work density obtained from constitutive equation (3): (a) second-order work density against ζ and η; (b) cross-section of the stability surface together with the failure surface and the bound surface on a deviatoric plane

procedure will be repeated until the stress satisfying equation (28) is found within a given tolerance.

In Figure 12(a) the second-order work density calculated from constitutive equation (3) is depicted against ζ and η. The stress state corresponding to Figure 12(a) lies inside the failure surface. It is seen from Figure 12(a) that d^2W is negative only for specific directions of stretching (the dark region in Figure 12(a)). Figure 12(b) shows the stability surface according to constitutive equation (3) together with the failure and the bound surface on a deviatoric plane. It can be concluded that for constitutive equation (3) the second-order work density may become negative before failure.

Now, let us investigate the physical meaning of the second-order work density. A simple but non-trivial case in a triaxial apparatus is the undrained test, where the specimen undergoes isochoric deformation. Making use of the triaxial stress state with $T_2 = T_3$ the second-order work density may be written as $\mathrm{d}^2W = \dot{T}_1 D_1 + 2\dot{T}_2 D_2$. It follows from $\mathrm{d}^2W = 0$ and incompressibility, $D_1 + 2D_2 = 0$, that $\dot{T}_1 - \dot{T}_2 = 0$, which means that the stress difference reaches its maximum. For loose sand, the maximum of the stress difference marks the beginning of strong reduction of the effective stress and hence the incipience of instability.

In spite of this simple and convincing example, the physical implication of $\mathrm{d}^2W = 0$ in general is less clear. Recently, Nova[35] investigated the controllability of tests with either stress or strain or both prescribed on the boundaries and found that the loss of controllability is associated with $\mathrm{d}^2W = 0$. A trivial case in a uniaxial test is that a stress control is impossible in the strain softening regime after the peak of the stress–strain curve. Strain softening is closely connected with the second-order work density. Here, we will consider strain softening as a material property. Most of the experimental studies are limited to strain softening behaviour in either triaxial tests with constant confining pressure or in uniaxial tests. For these simple cases, strain softening is often referred to as the so-called post-failure strain softening. After Valanis[33] a material element under uniform stress $\mathbf{T}$ and subjected to homogeneous straining is said to exhibit strain softening if the second-order work density is negative. According to this definition

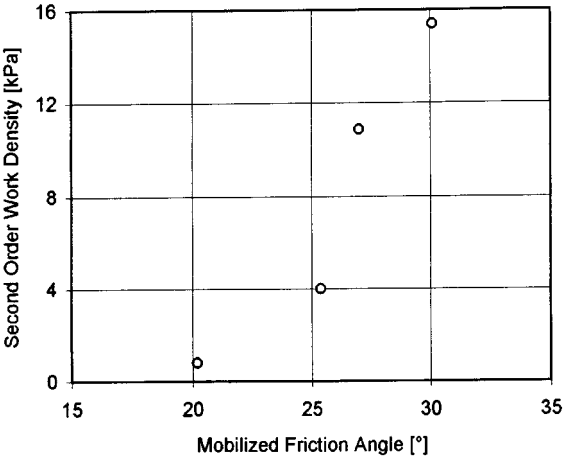

Figure 13. Second-order work density over mobilized friction angle obtained from a series of triaxial tests on specimens of dense sand

the stability surface is also the boundary for strain softening. Recent experiments on sand by Lade *et al.*[36] and by Chu and Lo[37] showed that there can be strain softening even prior to failure and called it *pre-failure strain softening*. This experimental finding agrees with the predictions of the hypoplastic model.

Triaxial tests are carried out on dense Karlsruhe medium sand with $e_0 \approx 0{\cdot}5$ to capture the stability surface for the case of triaxial stress states with $T_2 = T_3$. The tests are similar to that described in Section 5 with the difference that the change of the stress path is initiated at a mobilized friction angle $\phi_m = \arcsin[(T_1 - T_2)/(T_1 + T_2)]$ before failure. If it is possible to have $d^2W < 0$, another test is carried out with a smaller mobilized friction angle at which the stress path is changed. The results are shown in Figure 13. The mobilized friction angle at which the second-order work density becomes zero is about $\phi_m \approx 20^\circ$. This agrees qualitatively with the prediction of the constitutive model.

A final remark is concerned with the stability criterion and its applicability to granular materials. The recent experimental work by Lade *et al.*[36] Chu and Lo[37] and our own tests show that stable behaviour can be observed even though $d^2W < 0$ and cast some shade on the definition of stability according to the sign of the second-order work for granular materials. We deem that there can be no universal stability criteria without considering the essential features of the constitutive models in concern. In fact, our knowledge on stability relies largely on incremetnally linear models. There is as good as nothing on stability for incrementally non-linear models. The recent work by Wu and Sikora[4] on localized bifurcation shows that the incremental non-linearity brings new perspectives, which are entirely different from that of incrementally linear models. On the other hand, comparison between experiments and stability criteria is a delicate issue, since minor cause, e.g. confinement of rubber membrane, end friction, self-weight, might have major effect.

7. CONCLUDING REMARKS

Several outstanding problems of modelling granular materials have been investigated within the realm of the hypoplastic constitutive model. According to the classification of the constitutive

models, some interesting features at failure have been shown with the help of the stiffness loci. The discussion about the bound surface might appear strange for researchers working with plastic constitutive models. Nevertheless, if the stress–strain behaviour of granular materials depends on the stress (strain) path, why should failure *per se* not also be path dependant. That stress moves on the failure surface is nothing but an assumption, which is somehow *ad hoc* and has then been taken for granted in plasticity theory. We should not become too attached to an established concept. At the present stage, it seems to be premature to draw definite conclusion on the existence of the bound surface for granular materials other than that investigated and the whole issue merits further investigation.

Our analysis concerning the stability surface has shown that the second-order work density may become negative prior to failure. This agrees qualitatively with our own experimental results and those reported in the literature. However, the physical implication of the stability surface and the practical relevance still remain to be explored. No doubt, the investigation on stability will gain increasing importance in the future, for there are intricate phenomena, e.g. instability of rapid granular flow, which still await a plausible theoretical explanation. The relation between the stability surface obtained herein and the stability in the propagation of acceleration waves is ongoing and the results will be presented in a forthcoming publication.

ACKNOWLEDGEMENT

W.W. is grateful to Lahmeyer International Ltd. for the generous support to complete this work.

REFERENCES

1. D. Kolymbas, *A Constitutive Theory for Soils and other Granular Materials*. Habilitation in German, Karlsruhe University, 1988.
2. W. Wu and D. Kolymbas, 'Numerical testing of the stability criterion for hypoplastic constitutive equations,' *Mech. Mater*., **9,** 245–253 (1990).
3. D. Kolymbas, 'An outline of hypoplasticity,' *Ing. Arch*., **61,** 143–151 (1991).
4. W. Wu and Z. Sikora, 'Localized bifurcation in hypoplasticity,' *Int. J. Eng. Sci*., **29,** 195–201 (1991).
5. W. Wu, 'Hypoplasticity as a mathematical model for mechanical behaviour of granular materials,' *Dissertation*, Karlsruhe University, 1992, (*in German*).
6. W. Wu and E. Bauer, 'A hypoplastic constitutive model for barotropy and pyknotropy of granular materials, in *Proc. Int. Workshop Modern Approaches in Plasticity*, Elsevier, Amsterdam, 1993, pp. 225–258.
7. W. Wu and E. Bauer, 'A simple hypoplastic constitutive model for sand,' *Int. j. numer. anal. methods geomech*., **18,** 833–862 (1994).
8. D. Kolymbas, I. Herle and P. Wolffersdorff, 'Hypoplastic constitutive equation with internal state variables,' *Int. j. numer. anal. methods geomech*., **19,** 415–436 (1995).
9. E. Bauer and W. Wu, 'A hypoplastic constitutive model for cohesive powders,' *Powder Technol*., **85,** 1–9 (1995).
10. W. Wu and A. Niemunis, 'Failure criterion, flow rule and dissipation function derived from hypoplasticity,' *Mech. Cohesive-Frictional Mater*., **1,** 145–163 (1996).
11. W. Wu, E. Bauer and D. Kolymbas, 'Hypoplastic constitutive model with critical state for granular materials,' *Mech. Mater*., **23,** 45–69 (1996).
12. J. Tejchman and W. Wu, 'Numerical simulation of shear band formation with a hypoplastic model,' *Comput. Geotech*., **18,** 71–84 (1996).
13. C. Truesdell and W. Noll, 'The nonlinear field theories of mechanics, in S. Flügge (ed.) *Encyclopedia of Physics*, III/1, Springer, Berlin, 1965.
14. R. Hill, 'Some basic principles in the mechanics of solids without a natural time,' *J. Mech. Phys. Solids*, **7,** 209–225 (1959).
15. C. Truesdell, 'Hypo-elastic shear,' *J. Appl. Phys*., **27,** 441–447 (1956).
16. A. Stutz, 'Comportment elasto-plastique des milieux granularien,' *Foundation of Plasticity*, Noordoff, Leiden, 1973, pp. 33–49.
17. M. A. Romano, 'A continuum theory for granular media with a critical state,' *Arch. Mech*., **20,** 1011–1028 (1974).

18. R. O. Davis and G. Mullenger, 'A rate-type constitutive model for soils with a critical state,' *Int. j. numer. anal. methods geomech.*, **2,** 255–282 (1978).
19. Z. P. Bazant, 'Endochronic inelasticity and incremental plasticity,' *Int. J. solids Struct.*, **14,** 691–714 (1978).
20. G. Gudehus, 'A comparison of some constitutive laws for soils under radially symmetric loading and unloading, in *Proc. 3rd Int. Conf. Numer. Methods Geomech.*, Balkema, Holland, 1979, pp. 1309–1323.
21. P. Royis, 'Interpolations and one-to-one properties of incremental constitutive laws,' *Eur. J. Mech.* (A/Solids), **8,** 385–411 (1989).
22. T. Tokuoka, 'Yield conditions and flow rules derived from hypo-elasticity,' *J. Ration. Mech. Anal.*, **42,** 239–252 (1971).
23. A. Niemunis, 'Hypoplasticity vs. elastoplasticity, selected topics,' in *Proc. Int. Workshop Modern Approaches in Plasticity*, Elsevier, Amsterdam, 1993, pp. 277–307.
24. S. B. Batdorf and B. Budiansky, 'A mathematical theory of plasticity based on the concept of slip', *NACA TN 1871*, 1949.
25. A. Sawczuk and P. Stutz, 'On formulation of stress–strain relations for soils at failure,' *ZAMP*, **19,** 770–778 (1968).
26. M. Goldscheider, 'Grenzbedingung und Fließregel von Sand,' *Mech. Resear. Comm.*, **3,** 463–468 (1976).
27. W. Wu, 'A unified integration formula for the perfectly plastic von Mises model,' *Int. j. numer. methods eng.*, **30,** 491–504 (1990).
28. R. Chambon, J. Desrues, W. Hammad and R. Charlier, 'CLoE, a new rate-type constitutive model for geomaterials theoretical basis and implementation,' *Int. j. numer. anal. methods geomech.*, **18,** 253–278 (1994).
29. W. Wu and D. Kolymbas, 'On some issues in triaxial extension tests', *ASTM Geotech. Testing J.*, **14,** 276–287 (1991).
30. R. Hill, 'On constitutive inequalities for simple materials—I,' *J. Mech. Phy. Solids*, **16,** 229–242 (1968).
31. R. Hill, 'On constitutive inequalities for simple materials—II,' *J. Mech. Phy. Solids*, **16,** 315–322 (1968).
32. Z. P. Bazant, 'Stable states and paths of structures with plasticity and damage,' *J. eng. mech. div. ASCE*, **114,** 2013–2034 (1988).
33. K. C. Valanis, On the uniqueness of solution of the initial value problem in softening materials, *J. appl. mech., ASME*, **52,** 649–653 (1985).
34. H. Petryk, 'Material instability and strain-rate discontinuities in incrementally nonlinear media,' *J. Mech. Phys. Solids*, **40,** 1227–1250 (1992).
35. R. Nova, 'Controllability of the incremental response of soil specimen subjected to arbitrary loading programmes,' private communication, 1995.
36. P. V. Lade, R. B. Nelson and Y. M. Ito, 'Instability of granular materials with nonassociated flow,' *J. eng. Mech. div ASCE*, **113,** 1302–1318 (1987).
37. J. Chu and S.-C. R. Lo, 'Asymptotic behaviour of a granular soil in strain path testing,' *Geotechnique*, **44,** 65–82 (1994).
38. P. Vermeer, 'A five constant model unifying well established concepts,' *Proc. Int. Workshop on Constitutive Relations for Soils*, Balkema, Holland, 1982, pp. 175–197.
39. D. C. Drucker, 'Discussion on nonassociated flow and stability of granular materials,' *J. eng. mech. div. ASCE*, **114,** 1842–1845 (1988).
40. R. Hill, 'Aspects of invariance in solid mechanics, in C. S. Yih (ed.), *Advances in Applied Mechanics*,' 8, Academic Press, New York, 1978, pp. 1–75.
41. C. Truesdell, 'Hypo-elasticity,' *J. Ration. Mech. Anal.*, **4,** 83–133 (1955).

